www.nature.com/ismej

ISME

ARTICLE OPEN

Changes in interactions over ecological time scales influence single-cell growth dynamics in a metabolically coupled marine microbial community

Michael Daniels[1,2,3]✉, Simon van Vliet[4] and Martin Ackermann[1,2]

Microbial communities thrive in almost all habitats on earth. Within these communities, cells interact through the release and uptake of metabolites. These interactions can have synergistic or antagonistic effects on individual community members. The collective metabolic activity of microbial communities leads to changes in their local environment. As the environment changes over time, the nature of the interactions between cells can change. We currently lack understanding of how such dynamic feedbacks affect the growth dynamics of individual microbes and of the community as a whole. Here we study how interactions mediated by the exchange of metabolites through the environment change over time within a simple marine microbial community. We used a microfluidic-based approach that allows us to disentangle the effect cells have on their environment from how they respond to their environment. We found that the interactions between two species—a degrader of chitin and a cross-feeder that consumes metabolic by-products—changes dynamically over time as cells modify their environment. Cells initially interact positively and then start to compete at later stages of growth. Our results demonstrate that interactions between microorganisms are not static and depend on the state of the environment, emphasizing the importance of disentangling how modifications of the environment affects species interactions. This experimental approach can shed new light on how interspecies interactions scale up to community level processes in natural environments.

The ISME Journal (2023) 17:406–416; https://doi.org/10.1038/s41396-022-01312-w

INTRODUCTION

Microorganisms contribute to global cycling of elements, host health and many industrial processes. Yet, we currently lack quantitative insight into the exact mechanisms of how interspecies interactions modulate the growth of individual community members, and how the growth of individual community members scales up to determine the activity and growth of the community [1]. Such insight would allow us to better understand how activities observed at the level of microbial communities emerge from processes at lower levels of organization.

Species in microbial consortia perform metabolic functions collectively: catabolic processes are often distributed across different species which interact through the exchange of intermediate metabolites through the environment [2]. This distributed metabolism is especially common for complex substrates whose degradation involves several enzymatic reactions [3]. In natural environments a major resource for microbial communities are natural polymers, such as cellulose and chitin [4]. These polymers are structural components of multicellular organisms (cellulose in plants and chitin in arthropods), and are released into the environment upon death of these organisms. A complex community of interacting species is typically formed on these polymers [5]. Specialized bacteria cleave polymers via extracellular enzymes into accessible subunits, i.e., sugar mono- or oligomers that are small enough to be imported into the cell [6]. This process builds the foundation of a trophic cascade that leads to the eventual remineralization of natural polymers. Some bacterial cells without the ability to degrade polymers are able to take up the degradation products from the surrounding environment [7]. These so-called consumers thus directly benefit from the presence of degraders. Other microbial species that lack the necessary enzymes for polymer degradation are additionally unable to catabolise the cleaved degradation products; they rely on excreted metabolic by-products as growth substrates [8]. This process is called cross-feeding.

Cross-feeding, or syntrophy, is an interaction in which one organism uses another organism's by-products as a resource [9, 10]. Cross-feeding is widely believed to underlie many mutualistic relationships between microbes, providing a driving force for the maintenance of diversity in microbial communities [11–13]. Cross-feeding can also be beneficial for the species that excretes the by-products [14]. Firstly, removing the product of biochemical reactions increases the reaction rate according to "Le Chatelier's principle" [15]. Secondly, cross-feeding can allow for the removal of toxic metabolic by-products that inhibit the growth of their producers [16, 17].

[1]Department of Environmental Systems Sciences, Microbial Systems Ecology Group, Institute of Biogeochemistry and Pollutant Dynamics, ETH-Zurich, Zurich, Switzerland. [2]Department of Environmental Microbiology, Eawag: Swiss Federal Institute of Aquatic Sciences, Duebendorf, Switzerland. [3]Interdisciplinary PhD Program Systems Biology, ETH-Zurich and University of Zurich, Zurich, Switzerland. [4]Biozentrum, University of Basel, Basel, Switzerland. ✉email: michael.daniels@eawag.ch

Received: 3 February 2022 Accepted: 23 August 2022
Published online: 7 January 2023

Interactions between species are generally classified as positive, negative, or neutral and are usually quantified by measuring the difference in yield or growth rate in co- vs. monocultures [18]. This approach assumes that interactions within communities remain constant during the time period over which they are measured. However, by consuming and releasing nutrients, cells dynamically change their environment. In turn, individuals alter their metabolic behavior to adjust to the changes they cause in their surroundings [19]. This process can cause metabolic interactions between species to change with time.

Cells respond to changes in the environment that are caused both by their own activity and by the activity of all other community members. This leads to a complex feedback loop where the state of the environment, the metabolic activity of the community members, and the interactions between all these members become interdependent [9]. In order to gain a mechanistic understanding of complex community dynamics, it is essential to disentangle how cells respond to their environment (i.e., the metabolites that other community members release) from the effect that these cells have themselves on their environment (i.e., through the uptake of metabolites). However, this cannot easily be done using traditional culturing techniques.

Here, we developed a novel microfluidics-based approach that allows us to analyze how changes in the environment, caused by the collective metabolic activity of a community, affects the growth dynamics of individual cells. Microfluidics enables us to decouple the response of a cell to its environment from the effect it has on the environment itself. This approach thus allows us to quantify how metabolic interactions between species change over time.

We apply our method to study interactions in a naturally derived community that utilizes the polymer chitin. This community consists of a degrader and a cross-feeding species: *Vibrio natriegens* and *Alteromonas macleodii*. *Vibrio natriegens* is a marine chitin degrader [20]. It secretes chitinolytic enzymes into the environment in order to cleave chitin oligomers into monomers and dimers that it can take up into the cell. *Alteromonas macleodii* is unable to degrade chitin [5]. Furthermore, it lacks the ability to consume chitin degradation products. As a cross-feeding species, it relies on excreted metabolic by-products produced by the degrader.

We find that the interaction between degrader and cross-feeder changes over time from mutualism to competition for excreted metabolic by-products. Furthermore, the initially positive interaction between degrader and cross-feeder leads to an increased enzyme activity on a community level compared to a situation where the degrader grows alone. Finally, we found that the growth rates of individual cells can show substantial variation, especially for cross-feeders during periods of low nutrient concentrations.

RESULTS AND DISCUSSION

Microfluidics-based approach to study interactions in microbial communities

We developed a novel microfluidics-based approach that allows us to investigate growth dynamics of single cells that experience an environment which is dynamically changing in response to the collective metabolism of a microbial community. In order to achieve this, we couple a mother machine device [21] to a community batch culture and follow cell growth using time-lapse microscopy (Fig. 1B). The microfluidic device contains the two members of a simple community consisting of *Vibrio natriegens*—the degrader—and *Alteromonas macleodii*—the cross-feeder (Fig. 1A). The device is connected to a feeding batch culture in a serum flask. We inoculate bacteria (either the degrader alone or the degrader and the cross-feeder) at low densities into these serum flasks containing sterile growth media and chitin polymer as a carbon source (Fig. 1C, D). As microbial cells in the feeding batch culture consume resources and grow, they transition from lag- to exponential to stationary growth phase. In this process they sequentially alter their environment in two major related fashions: the initially available nutrients are consumed by the community members, while new nutrients—such as metabolic by-products—become available via the release of metabolites into the environment. The uptake and release of metabolites constantly changes the biochemical environment within the batch culture and consequently in the attached microfluidic device. Cells in the microfluidic device are thus exposed to the same—temporally changing—metabolic environment as the community in the batch culture, but as they are located downstream they cannot change the environment. This approach thus allows us to disentangle how metabolic interactions within microbial communities change over time. Previous studies have used similar approaches in order to answer fundamental questions about microbial physiology in clonal populations [22–25]. Here, we use this approach to study the growth dynamics of individual cells in simple microbial communities.

We first studied the growth dynamics in the metabolic environment created by the full cross-feeding community consisting of both the degrader and the consumer. We inoculated the batch culture with both species and followed the growth over a full cycle (i.e., from lag, via exponential, to stationary phase). In the feeding batch culture, the degrader releases lytic enzymes into the environment and consumes the chitin oligomers. During this process the degrader releases metabolic by-products into the environment which are in turn consumed by the cross-feeder. We analyzed the growth dynamics of the individual species by measuring the growth rates of single cells in the microfluidics device. Both the cross-feeder and the degrader start growing nearly instantaneously after the batch culture is inoculated (Fig. 2). This indicates that nutrients for cross-feeding are released as soon as the degraders start with the degradation of chitin. As cells grow and nutrients are depleted both species transition into the stationary phase where their growth rates approach zero. For the degrader growth stops around 25 h while for the cross-feeder growth continues until 40 h (Fig. 2). The difference in the duration of the growth phase can be explained by differences in metabolic niches. While the degrader primarily grows on chitin degradation products [26] the cross-feeder can utilize at least one metabolic by-product excreted by the degrader [27].

Interactions between degraders and cross-feeders are time dependent

We observed that growth rates changed in a non-monotonic way over time (Fig. 2); this raises the question whether metabolic interactions between degraders and cross-feeders change with time and how this affects the growth of the degrader. To address this question, we measured the single-cell growth dynamics of degrader cells in two different environments. Specifically, we fed degrader cells with two different batch cultures; one culture contained a co-culture of degrader and cross-feeder (Fig. 2) while the second culture contained the degrader in mono-culture.

We found that the growth dynamics of the degrader in these two conditions differed in two major ways (Fig. 3A): initially the growth rate of the degrader was higher in the presence of the cross-feeder. In the presence of the cross-feeder the degrader showed a 11% increase in growth rate during the first 20 h. This indicates that the cross-feeder facilitates the degrader's growth in the initial stages of their metabolic interaction (Fig. 3A, C). At later stages degrader cells in mono-culture exhibit a clear secondary growth phase (Fig. 3A). This growth phase is missing in the co-culture environment. Degrader cells in the mono-culture environment grow at higher rates in this secondary growth phase than individuals that experience a co-culture environment. In the absence of the cross-feeder the degrader had a growth rate that was about 173% higher during the secondary growth phase. Growth during the secondary growth

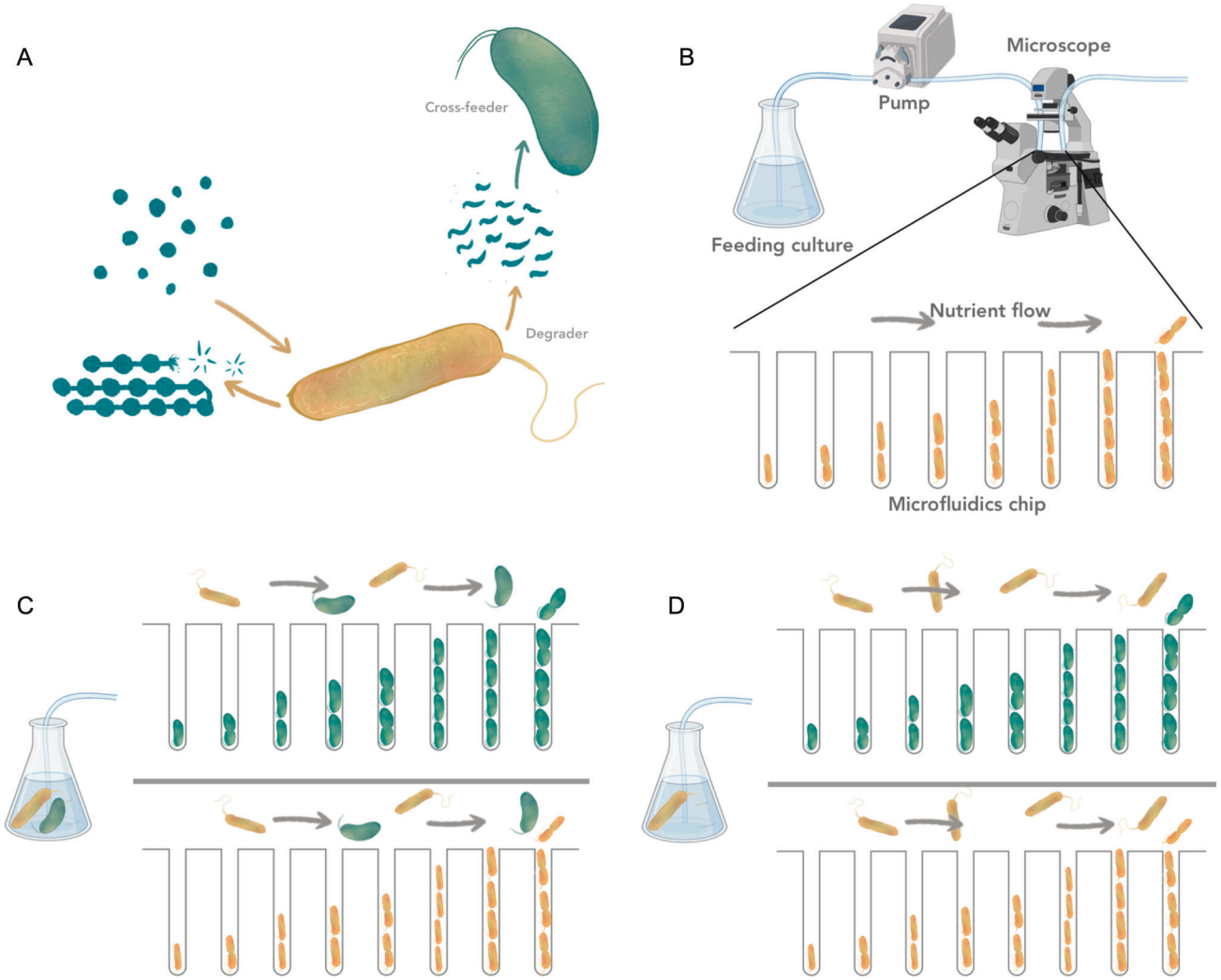

Fig. 1 Quantifying the temporal effects of interaction on single-cell growth dynamics. A Schematic illustration of the metabolic interactions between the degrader (*V. natriegens*, yellow) and the cross-feeder (*A. macleodii*, green) in a situation where chitin is the only available carbon source. **B** Microfluidic setup to quantify the growth dynamics of single cells that experience a batch culture environment. Bacteria are grown in a microfluidic device and are monitored using time-lapse microscopy. The device is connected to a batch culture containing nutrients and bacteria. Via a peristaltic pump, a small proportion of the feeding culture is constantly flushed through the microfluidic chip. Single cells in the microfluidic device experience the same environment as the cells in the feeding batch culture. By the consumption of nutrients and excretion of metabolic by-products, cells in the batch culture change the environment. Cells in the microfluidics device will respond to the change in environment, i.e., via changes in growth rate, but cannot change the environment themselves. **C**, **D** The microfluidic chips consist of several independent main channels. Each channel is loaded with one of the two species that constitute the community and connected to a single batch culture that contains either the full community with both species (**C**) or only the degrader species (**D**). By comparing single-cell properties from various batch-microfluidics combinations we can study how the presence of species in communities affect others and themselves. Images were adjusted from BioRender and partially provided by Daniel J. Kiviet.

phase leads to higher overall biomass accumulation in degrader cells that experienced a mono-culture environment without cross-feeders at the end of the 40 h experiment (Fig. 3B, D). The secondary growth phase can be explained by the reuptake of previously excreted metabolic by-products and corresponds to the diauxic shift observed in various microbiological systems [28, 29].

Our data reveal a shift in interactions between the degrader and the cross-feeder over ecological time scales: over the course of the growth period the effect of the cross-feeder on the degrader turns from positive to negative. Initially, the cross-feeder facilitates growth, possibly through the removal of growth inhibitory or production of growth promoting metabolites, which positively influences growth of the degrader. At later stages, the presence of the cross-feeder decreases growth of the degrader, possibly because the two types of organisms compete for metabolic by-products. Our data suggest that degrader cells release metabolic by-products into the media during growth on the polymers (first growth phase), an interpretation that we test and support below. Some of these by-products can be consumed by both the degraders and cross-feeders, however the cross-feeder consumes the released by-products constantly, and as a result degrader cells no longer show a second growth phase when cross-feeders are present. These results show that interactions between community members can change over short ecological time scales.

Interaction is governed by acetate excretion and consumption

Our findings that the degrader is able to display a second growth phase in mono-culture but not in co-culture with the cross-feeder, raise the question about which metabolite, or which metabolites, are primarily driving the metabolic interaction between the degrader and the cross-feeder. A common interaction mechanism in marine microbial communities is the production and

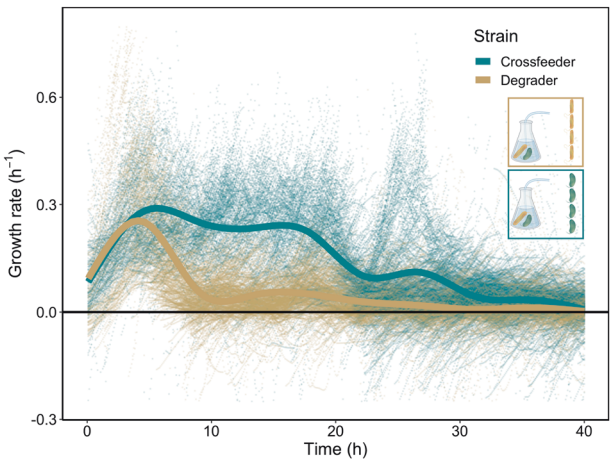

Fig. 2 Degrader and cross-feeder cells differ in their growth dynamics when experiencing a co-culture environment. Degrader (yellow) and cross-feeder (green) cells in microfluidic devices were connected to a growing batch culture containing a co-culture of the degrader and the cross-feeder. In the batch culture cells were growing in minimal medium containing 0.1% (w/v) Chitopentaose. Single-cell growth rates (points) of each cell present were plotted as a function of time. Lines represent the smoothed means (geom_smooth, ggplot2, RStudio) at each time interval using a generalized additive model. As chitin is degraded via secreted enzymes, resources become available and both cell types start growing. Cross-feeders grow for a longer time before growth rates drop to zero. Four replicate experiments were performed. In total 5608 individual cells were analyzed ($N_{(Degrader)} = 1707$; $N_{(Cross\text{-}feeder)} = 3901$). This leads to 270,677 instantaneous single-cell growth rates ($N_{(Degrader)} = 140{,}126$; $N_{(Cross\text{-}feeder)} = 130{,}551$). 1363 ($N_{(Degrader)} = 1086$; $N_{(Cross\text{-}feeder)} = 274$) data points are not shown because they fall out of the axis range.

consumption of acetate [30]. In order to test whether acetate production and consumption play a role in the interactions between the degrader and the cross-feeder in our system, we measured acetate concentrations of mono- and co-cultures over time. First, we investigated whether acetate levels vary between the mono- and co-culture at different time points. We found that absolute acetate levels in the media increase at first in the experiment (Fig. 4A). This indicates that acetate production is a metabolic by-product of the initial chitin degradation. The acetate levels change over time in the two batch culture conditions. In co-culture acetate concentrations reach lower peak levels and are overall lower when corrected for population size (Fig. 4B). These findings show that the cross-feeder is constantly consuming a fraction of the produced acetate. In the degrader mono-culture acetate accumulates in the early phases and declines at later time points. This indicates that, given the opportunity, the degrader will consume previously released acetate which leads to the secondary growth. Second, we wanted to verify whether both cell types were able to utilize the accumulated acetate. We found that both members of the community will consume acetate if they are growing on spent media from either mono- or co-culture batch (Fig. 4C). Taken together, our results indicate that during the initial phases of chitin degradation acetate is produced as a metabolic by-product. In mono-culture the degrader produces acetate in the early phases of the experiment while chitin is still available and consumes acetate when the primary resource has been depleted (Fig. S4). In co-culture the cross-feeder constantly consumes part of the acetate. This prevents a secondary growth phase of the degrader in co-culture condition. Our data show that acetate released by the degrader is an important nutrient source for the cross-feeder; however, additional metabolites could also play a role in the cross-feeding interaction and further work is needed to uncover the full scope of metabolic interactions. While acetate is a common metabolite involved in metabolic cross-feeding, the plethora of metabolites likely to be released by the degrader are not characterized in our study. Therefore, it is important to note that the precise metabolic interactions in this system are not known.

Presence of cross-feeder influences degrader's ability to degrade polymer

In microbial systems that rely on polymer degradation for nutrient availability, growth and enzyme production are tightly coupled: increases in enzyme production and activity increases the concentration of assimilable breakdown products and hence the potential for growth. Since the degrader's growth rate is initially increased in the presence of the cross-feeder (Fig. 3) we investigated whether the cross-feeders increase total enzyme activity in the degraders (either through an increase in the amount that is produced or by an increase in the catalytic activity per enzyme molecule). To this end we measured total enzyme activity when the degrader was growing alone and when it was growing in the presence of the cross-feeder. Using a commercially available enzyme assay kit, we measured the specific activity of chitinases in cell free supernatants. We found that in co-culture chitinase activity is increased when compared to a degrader mono-culture (Fig. 5). The cross-feeder does not have any enzymes that cleave the polymer chitin (Fig. S1); instead our data show that the presence of the cross-feeder increased the total enzyme activity in the degrader cells. We normalized the enzymatic activity using the total OD of the community. As part of the community consists of cross-feeder cells we thus underestimate the chitinase activity per unit of degrader biomass.

Higher enzymatic activity can originate in two ways. It is plausible that the effect is a consequence of the removal of metabolites (i.e., through cross-feeding) that reduce the catalytic activity of the enzymes themselves. Alternatively, other effects such as an increase in enzyme production by the degrader are also possible. Our data thus suggests that the cross-feeder is able to influence the community level function of chitin degradation by increasing enzyme activity in the degrader. Increased activity of lytic enzymes will generally lead to increases in availability of chitin degradation products and therefore higher growth rates for the degrader. We will be addressing the exact mechanism of this phenomenon in a future study.

Effect of cross-feeder on its own growth dynamics

We observed that the cross-feeder increases the growth and chitinase activity of the degrader cells. This raises the question whether the cross-feeders receive an indirect benefit from this interaction, through their promotion of the degrader's growth and the resulting increase in metabolic by-products. Here we address this question by measuring single-cell growth dynamics of cross-feeder cells supplied with nutrients from two different feeding batch cultures. One culture contained a co-culture of degrader and cross-feeder (Fig. 2) while the second culture contained the degrader in mono-culture.

In co-culture the cross-feeder behaves as in a natural community where it can interact with the degrader e.g., by stimulating enzyme activity. When connected to a mono-culture, the cross-feeder experiences an environment that is purely shaped by the degrader. Individual cross-feeder cells in the microfluidics device react to metabolic processes of the degrader population in the feeding batch culture without being able to influence them. The natural equivalent of this system would be a community where the cross-feeder is so rare that its presence does not alter the degrader's behavior while still being able to consume excreted metabolic by-products. Using this approach, we quantify if the cross-feeder grows better when it is able to interact with the degrader and affects the environment through its presence.

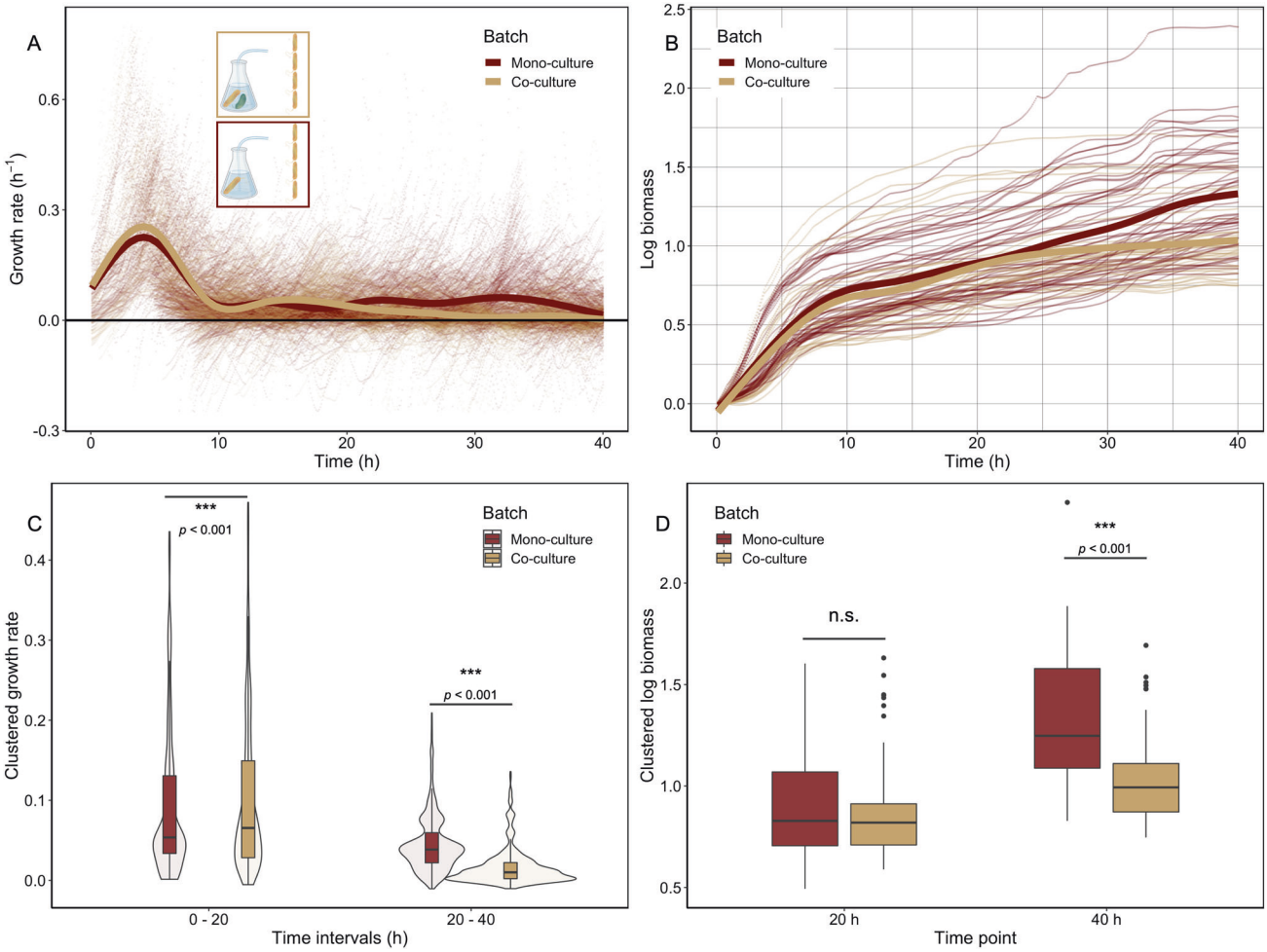

Fig. 3 Growth of the degrader is affected by the presence of the cross-feeder in a time dependent manner. Degrader cells in microfluidic chips were connected to two different batch cultures: one with degrader cells in mono-culture (red) and one with a co-culture of degrader and the cross-feeder (yellow). **A** Single-cell growth rates (points) are plotted as a function of time. Lines represent the smoothed means (geom_smooth, ggplot2, RStudio) using a generalized additive model. During the first hours the degrader cells supplied with co-culture media grow faster than cells experiencing a mono-culture environment. At later time points we observe a marked secondary growth phase for cells fed by mono-culture that is absent for cells fed by co-culture. Four replicate experiments were performed. Overall 99 mother machine channels were analyzed ($N_{(\text{Co-culture})} = 49$; $N_{(\text{Monoculture})} = 51$). In total 3934 individual cells were analyzed ($N_{(\text{Mono-culture})} = 2227$; $N_{(\text{Co-culture})} = 1707$). 1494 ($N_{(\text{Mono-culture})} = 405$; $N_{(\text{Co-culture})} = 1089$) data points are not shown because they fall out of the axis range. **B** Biomass accumulation of degrader cells when experiencing a mono- or co-culture environment. Cells that experience a co-culture environment (yellow) tend to grow to higher yields in the first 20 h than cells that experience a mono-culture environment (red). Due to benefits of the secondary growth phase, cells in mono-culture seem to reach higher overall yields at the end of the experiment. **C** Comparison of average growth rate of degrader cells between the two main growth phases. Single-cell growth rates were averaged for each time point (Fig. S2) and binned into two 20 h time windows. During the first 20 h the single-cell growth rates were significantly higher when the degrader experienced a co-culture environment (red) compared to a mono-culture condition. Analysis using a mixed effect model (with the fixed effect culture-type and the random effect day of the experiment) revealed significant higher growth rates for the co-culture condition; ($N_{(\text{Co-culture})} = 956$; $N_{(\text{Monoculture})} = 956$, growth rate difference = 0.09, std.Error = 0.02, $p \ll 0.001$). The growth rate in this phase was 11.1% (±2.6%, standard error SE) higher for the co-culture condition. Growth during the secondary growth phase is significantly higher in mono-culture; ($N_{(\text{Co-culture})} = 956$; $N_{(\text{Monoculture})} = 956$, growth rate difference = 0.52, std.Error = 0.02, $p \ll 0.001$). The growth rate in this phase was 173.3% (±7.4%, SE) higher for the mono-culture condition. **D** Comparison of total cell growth for both batch culture conditions at two time points. For each microfluidic mother machine biomass accumulation was calculated (see Methods). During the primary growth phase degrader cells showed no statistical difference in biomass accumulation. Analysis using a mixed effect model (with the fixed effect culture-type and the random effect day of the experiment) revealed no statistically-significant difference in biomass accumulation between co-culture and mono-culture after 20 h ($N_{(\text{Co-culture})} = 49$; $N_{(\text{Monoculture})} = 51$, difference in biomass = 0.06, std.Error = 0.03, $p = 0.06$). The degrader accumulated 1.1% (±1.1%, SE) more biomass in the first 20 h in the mono-culture condition. After 40 h analysis using a mixed effect model (with the fixed effect culture-type and the random effect day of the experiment) revealed a statistically-significant difference in biomass accumulation between mono-culture and co-culture. ($N_{(\text{Co-culture})} = 49$; $N_{(\text{Monoculture})} = 51$, difference in biomass = 0.22, std.Error = 0.04, $p \ll 0.001$). The degrader had accumulated 26.2% (±4.6%, SE) more biomass at the end of the 40 h experiment in the mono-culture condition.

We find that during the first 20 h the positive effect the cross-feeder has on the growth dynamics of the degrader is not reflected in increased growth rate (Fig. 6A, C) or biomass production of itself (Fig. 6B, D). During this time the cross-feeder displayed an ~7% increase in single-cell growth rate when connected to a degrader mono-culture batch. This could indicate that the nutrients required for growth are limited as the cross-feeder cells constantly consume the excreted metabolites. At later time points, we observe high single-cell growth rates and biomass accumulation for the cross-feeder cells that experience a degrader

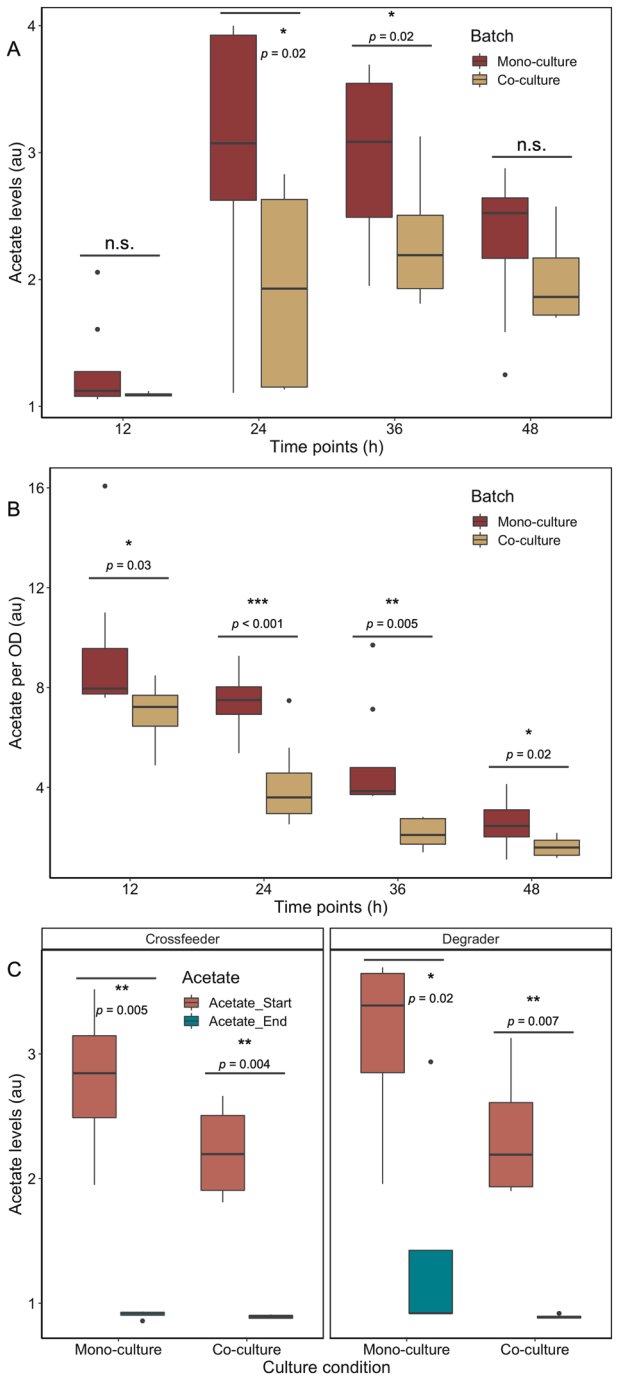

Fig. 4 Acetate levels govern cross-feeding interactions. Acetate concentrations measured in batch cultures at various time points. **A** Acetate levels for degrader mono-culture (red) and co-cultures (yellow) in batch cultures change over time. The presence of the cross-feeder leads to lower overall acetate levels. (Welch two sample *t*-test; $N = 8$; 12 h: mean of mono-culture = 1.29 FU, mean of co-culture 1.09 FU; $t = 1.50$, p value = 0.09, 24 h: mean of mono-culture = 2.95 FU, mean of co-culture 1.93 FU; $t = 2.17$, p value = 0.02, 36 h: mean of mono-culture = 2.95 FU, mean of co-culture 2.28 FU; $t = 2.23$, p value = 0.02, 48 h: mean of mono-culture = 2.31 FU, mean of co-culture 2.00 FU; $t = 1.27$, p value = 0.11). **B** Acetate levels per OD for degrader mono-culture (red) and co-cultures (yellow) in batch cultures change over time. In the early phases, relative acetate concentration per OD is higher. (Welch two sample *t*-test; $N = 8$; 12 h: mean of mono-culture = 9.39 FU, mean of co-culture 6.94 FU; $t = 2.14$, p value = 0.03, 24 h: mean of mono-culture = 7.43 FU, mean of co-culture 4.11 FU; $t = 4.22$, p value « 1e−3, 36 h: mean of mono-culture = 4.96 FU, mean of co-culture 2.15 FU; $t = 3.42$, p value = 0.005, 48 h: mean of mono-culture = 2.58 FU, mean of co-culture 1.61 FU; $t = 2.38$, p value = 0.02). **C** Degrader and cross-feeder cells can consume available acetate. When degrader and cross-feeder are grown on spent media from batch cultures, acetate levels before growth (red) and after 48 h of growth (green) vary. (Welch two sample *t*-test; $N = 4$; cross-feeder on mono-culture: mean of acetate at start = 2.79 FU, mean of acetate at end 0.91 FU; $t = 5.69$, p value = 0.005; cross-feeder on co-culture: mean of acetate at start = 2.22 FU, mean of acetate at end 0.89 FU; $t = 6.50$, p value = 0.004; degrader on mono-culture: mean of acetate at start = 3.11 FU, mean of acetate at end 2.15 FU; $t = 2.61$, p value = 0.02; degrader on co-culture: mean of acetate at start = 2.35 FU, mean of acetate at end 0.89 FU; $t = 5.12$, p value = 0.007).

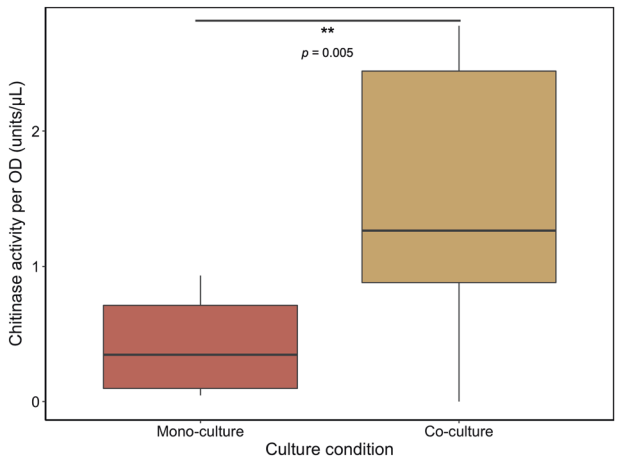

Fig. 5 Cross-feeder influences degrader's chitinase activity. Chitinase activity per unit OD (optical density) in exponential growth phase in minimal media with 0.1% Chitopentaose (w/v). The presence of a cross-feeder significantly increases the overall chitinase activity of the community Mixed effect model (with the fixed effect culture-type and the random effect day of the experiment) revealed significant chitinase activity for the co-culture condition; $N_{(Co\text{-}culture)} = 8$; $N_{(Monoculture)} = 8$, difference in chitinase activity = 1.0, std.Error = 0.36, $p = 0.005$). Chitinase activity was 241.2% (±85.7%, SE) higher for the co-culture condition.

mono-culture condition (Fig. 6A–D). During this time the cross-feeder displayed a 211% increase in single-cell growth rate when it was not part of the feeding culture. This difference in growth dynamics between mono- and co-culture can be explained by intraspecies competition. When the cross-feeder is part of the community, cross-feeder cells in the feeding culture consume metabolites and thereby reduce the access to these metabolites for the cross-feeder in the microfluidic device. This means that in a co-culture environment cross-feeders experience intraspecies competition. This competition is absent in a degrader mono-culture environment. Taken together, our data thus suggests that the presence of cross-feeders in the community leads to rapid depletion of metabolic by-products and therefore increased intraspecies competition.

Distribution of single-cell growth rates depend on environment and interactions

Previous studies have shown that cell growth rates can vary strongly between individual cells in a population [31]. This variation in growth rate can either be caused by variation in the micro-environments of cells [32], or by stochastic fluctuations [33]. One advantage of our microfluidic approach is that we can directly

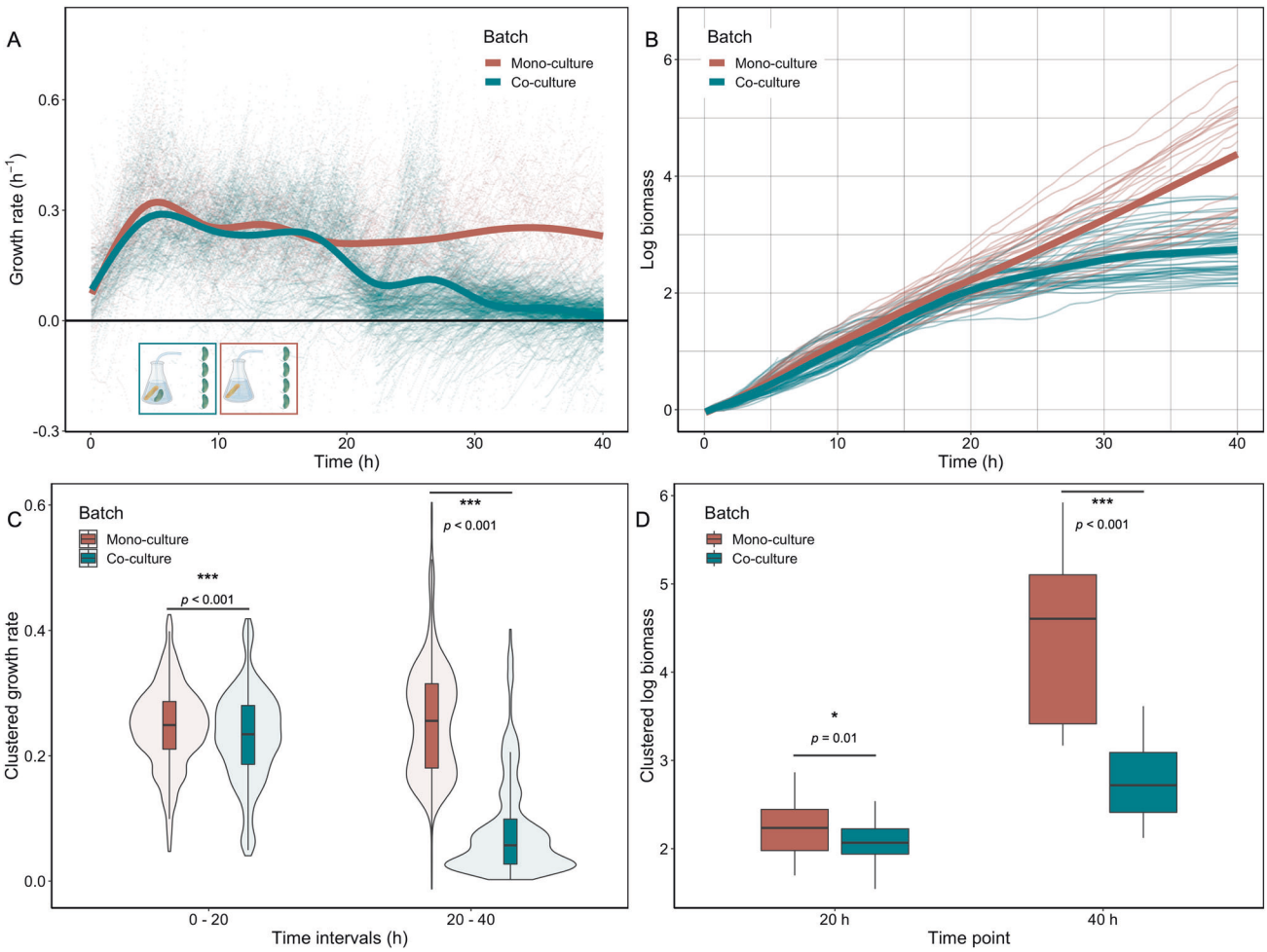

Fig. 6 Cross-feeders' growth dynamics are dominated by intraspecies competition. Cross-feeder cells in microfluidic chips were connected to two different batch cultures: one with degrader cells in mono-culture (red) and one with a co-culture of degrader and the cross-feeder (green). **A** Single-cell growth rates (points) are plotted as a function of time. Lines represent the smoothed means using a generalized additive model. Initially, cross-feeder cells showed comparable growth trajectories for both environments. As cross-feeder cells in the co-culture consume metabolites excreted by the degrader they use up their available resources and growth rates for cells in the microfluidics device eventual declines. In the degrader mono-culture environment there are no cells that consume all of the previously released metabolic by-products. Under this condition cells in the microfluidics device can grow constantly as they do not experience competition for nutrients. Four replicate experiments were performed. Overall 100 mother machine channels were analyzed ($N_{(\text{Co-culture})} = 60$; $N_{(\text{Monoculture})} = 40$). In total 6558 individual cells were analyzed ($N_{(\text{Mono-culture})} = 2657$; $N_{(\text{Co-culture})} = 3901$). 322 ($N_{(\text{Mono-culture})} = 48$; $N_{(\text{Co-culture})} = 274$) data points are not shown because they fall out of the axis range. **B** Biomass accumulation of cross-feeder cells when experiencing a mono- or co-culture environment. In the first 20 h, cells in the two conditions accumulate biomass at the same rate. For cross-feeder cells experiencing a co-culture environment, biomass starts to plateau at the 20 h mark. Single cells connected to a degrader mono-culture batch accumulate biomass at a constant rate until the end of the experiment. **C** Comparison of average growth rate of cross-feeder cells between the two main growth phases. Single-cell growth rates were binned into two 20 h time windows. During the first 20 h the single-cell growth rates were significantly higher when the cross-feeder experienced a degrader mono-culture environment compared to cells that experienced a co-culture environment. Analysis using a mixed effect model (with the fixed effect culture-type and the random effect day of the experiment) revealed significant higher growth rates for the mono-culture condition; ($N_{(\text{Co-culture})} = 956$; $N_{(\text{Monoculture})} = 956$, growth rate difference = 0.04, std.Error = 0.01, $p \ll 0.001$). The growth rate in this phase was 6.8% (±1.2%, SE) higher for the mono-culture condition. At later stages growth during the secondary growth phase is significantly higher for cells connected to a degrader mono-culture (Mixed effect model (with the fixed effect culture-type and the random effect day of the experiment) revealed significant higher growth rates for the co-culture condition; $N_{(\text{Co-culture})} = 956$; $N_{(\text{Monoculture})} = 956$, growth rate difference = 0.64, std.Error = 0.01, $p << 0.001$). The growth rate in this phase was 210.5% (±4.1%, SE) higher for the mono-culture condition. **D** Comparison of total cell growth for both batch culture conditions for two time intervals. For each microfluidic mother machine biomass accumulation was calculated (see Methods). Analysis using a mixed effect model (with the fixed effect culture-type and the random effect day of the experiment) revealed statistically-significant difference in biomass accumulation between co-culture and mono-culture after 20 h ($N_{(\text{Co-culture})} = 60$; $N_{(\text{Monoculture})} = 40$, biomass difference = 0.14, std.Error = 0.06, $p = 0.01$). The cross-feeder accumulated 7.5% (±3.0%, SE) more biomass in the first 20 h in the mono-culture condition. During the later stages, cells that experience the mono-culture environment accumulate more biomass. Analysis using a mixed effect model (with the fixed effect culture-type and the random effect day of the experiment) revealed statistically-significant difference in biomass accumulation between co-culture and mono-culture after 20 h ($N_{(\text{Co-culture})} = 60$; $N_{(\text{Monoculture})} = 40$, biomass difference = 1.58, std.Error = 0.12, $p \ll 0.01$). The cross-feeder accumulated 59.7% (±4.5%, SE) more biomass in the mono-culture condition.

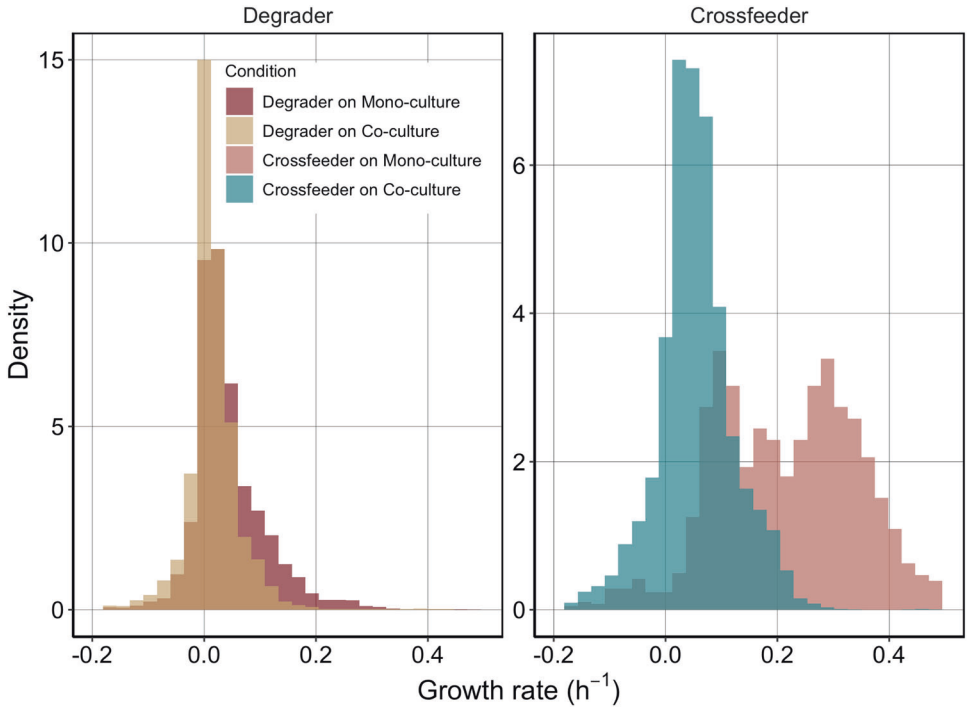

Fig. 7 Variation of single-cell growth rates. Variation of single-cell growth rates differ for degrader and cross-feeder under different conditions. **A** Density distributions of single-cell growth rates for the degrader on co-culture (yellow) and mono-culture (dark red) between 34–36 h. Degrader on Mono-culture: cv = 1.50, var = 0.004, Degrader on Co-culture cv = 4.24 var = 0.003. Bimodality calculations reveal no bimodal growth for either condition. (Hartigan's dip statistics, co-culture: $D = 0.003$, $p = 0.99$, mono-culture: $D = 0.003$, $p = 0.99$). **B** Density distributions of single-cell growth rates of cross-feeder on co-culture (green) and mono-culture (light red) between 34–36 h. Coefficient of variation (cv) and variance of distributions (var) show clear differences between these two conditions. Cross-feeder on Mono-culture: cv = 0.61 var = 0.018, cross-feeder on Co-culture CV = 1.37 var = 0.005. Calculation for bimodality using Hartigan's dip test show a clear bimodal distribution for the cross-feeder when growing on degrader mono-culture ($D = 0.02$, $p < 0.001$) but not for growth on co-culture ($D = 0.004$, $p = 0.75$).

measure this variation in cell growth rates and assess if and how it depends on interspecies interactions.

We investigated whether variation in cell growth rates and the distribution of cell growth rates depends on the interspecies interactions. We found that the degrader has generally narrower distributions than the cross-feeder (Fig. 7). The growth rate distributions of the degrader cells do not vary much between growth conditions, but they do change over time (Figs. S5 and S6). In contrast, for the cross-feeder we observed a strong change in the shape of the growth rate distribution between mono- and co-culture conditions at later time points (Fig. S5): in mono-culture conditions growth rates at later time points show a bimodal distribution (Fig. 7) with one fast and one slow growing subpopulation. This indicates that if the cross-feeder is rare (mimicked by the mono-culture set-up), part of the population can achieve high growth rates late in the growth season; presumably on metabolic by-products that still occur at substantial concentrations. A second part of the population appears to not grow or grows rather slowly. In co-culture conditions this fast-growing subpopulation is not present, and overall cell growth rates follow a more narrow distribution. This emergence of phenotypic heterogeneity in growth rates between genetically identical cells later in the growth cycle is in line with previous observations of how nutrient limitation can promote growth differences in clonal populations [32].

CONCLUSION

Our quantitative single-cell measurements of cells in a community context allows us to ask fundamental questions in microbial systems ecology that are usually difficult to experimentally tackle. (1) How is one species' growth dynamics affected by the presence of another species? (2) How do interactions between species in microbial communities change over time? (3) Do species benefit from the effects they have on others?

We showed that interactions change over ecological times: during early stages cross-feeders increase the growth of degraders—by increasing catalytic activity of individual enzymes or by inducing an increase in chitinase expression—while at later stages they decrease the growth of degraders—by outcompeting them for metabolic by-products, such as acetate. Overall, cross-feeders thus had a negative impact on the growth of degraders. Moreover, we showed that the growth of cross-feeders is primarily affected by intraspecies competition for resources.

In natural ecosystems, metabolic interactions are ubiquitous. Frequently, they are observed when cells colonize and degrade natural polymers such as cellulose or chitin where extracellular enzymes are utilized to digest them into subunits that can be taken up into the cell [6]. In these environments, non-lytic species cross-feed on metabolic by-products excreted by polymer degraders. Microbial communities that colonize these polymeric particles follow successional dynamics [5]. Diverse microbes with varying metabolic capabilities colonize marine particles at different points in time. We studied the cross-feeding that occurs in such natural systems using a small community. We observed that besides long-term successional patterns, interactions that change on short time-scales influence community level properties in these consortia. In future work, our system could easily be extended to more complex communities. For example, one could study the effect that a focal species has on the community dynamics by using batch cultures with and without this focal species and quantify the growth of all community members using the microfluidic device (with one species per channel). Microfluidics allows for relatively straightforward parallelization and communities with up to ~6–8 members could potentially be investigated using current tools. In addition, it would be interesting

to explore the dependence of the community dynamics on the initial fraction of the two cell types.

Our findings raise important questions about the predominant nature of microbial interactions in natural environments. In nature, polymer degrading microbial communities are subjected to chemo-physical factors. Diffusion or local flow in marine ecosystems might prevent the accumulation of excreted metabolic by-products. This would reduce the degrader's ability to consume previously released metabolites. Therefore, the interactions between degrader and cross-feeder might be more steered toward positive facilitation and syntropy.

These results highlight the importance of including the contribution of interspecies interactions in general and their temporal dynamics in particular into ecosystem scale models. Eventually, these findings might help us in engineering microbial communities relevant to our and our ecosystems well-being.

MATERIAL AND METHODS

Bacterial strains, media and batch cultures

We used the wildtype strain *Vibrio natriegens* ATCC 14048 and *Alteromonas macleodii* sp. 4B03 (non-clumping variant) isolated from marine particles [8]. Strains were cultured in Marine Broth (MB, Difco 2216) and grown overnight at 25 °C. In total, 1 ml of cell culture was centrifuged (13,000 rpm for 2 min) in a 1.5 ml microfuge tube. After discarding the supernatant, the cells were washed with 1 ml of MBL minimal medium medium without carbon source. Cells were centrifuged again and the cell pellet was resuspended in 1 ml of MBL (marine minimal medium) [30, 34] adjusted to an 0.002 OD600. Cells from these cultures were used for experiments in MBL minimal medium containing 0.1% (weight/volume) Pentaacetyl-Chitopentaose (Megazyme, Ireland). The carbon source was added to the MBL minimum medium and filter sterilized using 0.22 µm Surfactant-Free Cellulose Acetate filters (Corning, USA). A total of 500 µl of the prepared cultures (250 µl + 250 µl for co-cultures) were added to 9.5 ml of MBL + 0.1 % chitopentaose (v/w) in serum flasks. This resulted in a starting OD of 0.0001. The flasks included a stirrer and were sealed with a rubber seal. Serum flasks were stored on a bench top magnetic stirrer (500 rpm) and connected to the microfluidics setup via Hamilton NDL NO HUB needles (ga21/135 mm/pst 2).

Microfluidics

Microfluidics experiments were performed as described previously [35–38]. Cell growth was imaged within mother machine channels of 25 × 1.4 × 1.26 µm (length × width × height). Within these channels, cells could experience the batch culture medium that diffused through the main flow channels. The microfluidic device consisted of a PDMS flow cell (50 µm/23 µm). The PDMS flow cell was fabricated by mixing the SYLGARD 184 Silicone Elastomer Kit chemicals 10:1 (w/v), pouring the mix on a master waver and hardening it at 80 °C for 1 h. The solid PDMS flow cell was cut out of the master waver and holes were pierced at both ends of each flow channel prior to binding it to a cover glass (Ø 50 mm) by applying the "high" setting for 30 s on the PDC-32G Plasma Cleaner by Harrick Plasma. The flow cell was connected via 40 mm Adtech PTFE tubing (0.3 mm ID × 0.76 mm OD) to a Ismatech 10 K Pump with 40 mm of Ismatech tubing (ID 0.25 mm, OD 0.90 mm) which again was connected via 80 mm Adtech PTFE tubing (0.3 mm ID × 0.76 mm OD) via a 5 mm short Cole-Parmer Tygon microbore tubing (EW-06418-03) (ID 0.762 mm OD 2.286 mm) connector tubing to a Hamilton NDL NO HUB needle (ga21/135 mm/pst 2) that was inserted into the feeding culture. During the whole experiment the pump flow was set to 1.67 µl/min (0.1 ml/h).

Time-lapse microscopy

Microscopy imaging was done using fully automated Olympus IX81 or IX83 inverted microscope systems (Olympus, Japan), equipped with a ×100 NA1.3 oil immersion, phase contrast objective, an ORCA-flash 4.0 v2 sCMOS camera (Hamamatsu, Japan), an automated stage controller (Marzhauser Wetzlar, Germany), shutter, and laser-based autofocus system (Olympus ZDC 1 and 2). Detailed information about the microscopy setup has been described by D'Souza et al. [39]. Channels on the same PDMS Chip were imaged in parallel, and phase-contrast images of each position were taken every 5 min. The microscopy units and PDMS chip were maintained at room temperature. All experiments were run at a flow rate of 0.1 ml h^{-1}, which ensures nutrients enter the chamber through diffusion. Four biological replicates were performed. These replicates consist of four independent microfluidics channels (two for each of the strains). These channels were connected to one of two independent batch cultures.

The microscopy dataset consists of 200 mother machine channels; 49 channels for the degrader on co-culture, 51 for the degrader on mono-culture, 40 for the cross-feeder on mono-culture and 60 for the cross-feeder on co-culture.

Image analysis

Image processing was performed using a modified version of the Vanellus image analysis software (Daan Kiviet, https://github.com/daankiviet/vanellus), together with Ilastik [40] and custom written Matlab scripts.

Movies were registered to compensate for stage movement and cropped to the region of growth channels. Subsequently, segmentation was done on the phase contrast images using Ilastik's supervised pixel classification workflow and cell tracking was done using the Vanellus build-in tracking algorithm.

After visual curation of segmentation and tracking for each mother machine and at every frame growth parameters were calculated using custom written matlab scripts [36]. Lengths of individual cells were estimated by finding the cell center line by fitting a third-degree polynomial to the cell mask; then the cell length was calculated as the length of the center line between the automatically detected cell pole positions (see Kiviet et al. [33] for details).

We quantified cell growth by calculating single-cell elongation rates r from measured cell length trajectories: $L(t) = L(0)\cdot e\hat{}(r\cdot t)$. Cell lengths and growth rates varied drastically over the time course of the experiment; we thus developed a robust procedure that can reliably estimate elongation rates both for large fast-growing cells as well as for small non-growing cells. We first log-transformed cell lengths, which were subsequently smoothed over a moving time window with a length of 5 h (60 time points). We used a second order local regression using weighted linear least squares (*rloess* method of Matlab *smooth* function) in order to minimize noise while maintaining sensitivity to changes in elongation rates. Subsequently the instantaneous elongation rate was estimated as the slope of a linear regression over a moving time window of 30 min (7 time points). Time points for which the fit quality was bad ($\chi^2 > 10^{-4}$) were removed from the analysis [32]. All parameters were optimized manually by visually inspecting the fitting procedure of many cell length trajectories randomly selected from across all replicates.

As cells are continuously lost from the mother machine channels it is non-trivial to calculate the total amount of biomass produced in the chip. We thus need to estimate this quantity from the observed single-cell elongation rates. Specifically, we estimated the total amount of biomass produced per individual mother machine until a given time point as:

$$B_T = e^{\Delta t \sum_{i=1}^{T} <r_i>}$$

Where $<r_i>$ is the average growth rate of all cells in a given replicate at time point i, and where Δt is the time interval between two timepoints. By using the average growth rate, we ignore the variation in growth rates between cells. However, it is difficult to calculate population growth when growth rates vary both with time and between cells and the current method still allows us to capture the overall effect of interactions on cell growth.

Datasets and statistical analysis

All microfluidics experiments were replicated four times. No cells were excluded from the analysis after visual curation. For *V. natriegens* 2227 cells were analyzed on mono-culture, and 1707 cells were analyzed on co-culture. For *A. macleodii* 2657 cells were analyzed on mono-culture, and 3901 cells were analyzed on co-culture. Each mother machine channel was treated as an independent sample. All statistical analysis was performed in Rstudio v1.2.5033. Percent increases were calculated using the relative differences of estimated between the corresponding values. For mixed effect models analysis the LmerTest package (Version 3.1-3) [41] with the following equation were used: $y \sim \text{Batch} + (1 \mid \text{Replicate})$ The Tukey Post hoc test was performed using the Multcomp package (Version 1.4-15) [42].

Chitinase assay

Degrader and Cross-feeder cells were cultured in Marine Broth (MB, Difco 2216) and grown overnight at 25 °C. In total, 1 ml of cell culture was

centrifuged (13,000 rpm for 2 min) in a 1.5 ml microfuge tube. After discarding the supernatant the cells were washed with 1 ml of MBL minimal medium medium without carbon source. Cells were centrifuged again and the cell pellet was resuspended in 1 ml of MBL adjusted to an 0.002 OD600. A total of 10 µl of cell culture was added to 190 µl of MBL containing 0.1% Chitopentaose (w/v). Cultures were grown to exponential phase in a plate reader (Eon, BioTek) at 25 °C. Cell free supernatants were generated by sterile filtering cultures using a multi-well filter plate (AcroPrep) into a fresh 96 well plate. Chitinase activity of cell free supernatants was measured using a commercially available fluorometric chitinase assay kit (CS1030, Sigma-Aldrich) following the protocol. In short, 10 µl of sterile supernatant was added to 90 µl of the assay mix. The solution was incubated in the dark at 25 °C for 40 min before measuring fluorescence (Excitation 360 nm, Emission 450 nm) in a plate reader (Synergy MX, Biotek). Logarithmic chitinase activity per OD600 was analyzed for eight replicates.

Chitinase activity in units per ml was calculated using a standard concentration. Using the following Formula: $\text{Units/ml} = \frac{(\text{FLU}-\text{FLUblank}) \times 1.9 \times 0.3 \times \text{DF}}{\text{FLUstandard} \times \text{time} \times \text{Venz}}$

Here, FLU indicates measured fluorescence, DF indicates the dilution factor, and *V* indicates the volume of the sample in ml [43].

Acetate assay

Cell cultures were prepared and grown in serum flasks as described above. At different time intervals 1 ml of culture was removed and OD600 was measured. Cultures were filter sterilized using 0.22 µm Surfactant-Free Cellulose Acetate filters (Corning, USA) into a 1.5 ml microfuge tube. Cell free supernatants were stored at −4 °C until they were used for acetate measurements. Acetate concentrations were measured using a colorimetric assay kit (MAK086, Sigma-Aldrich) following the protocol. In short, 50 µl of cell free supernatant was added to 50 µl of assay mix. The solution was incubated in the dark at 25 °C for 30 min. Acetate concentrations were measured in a plate reader (Eon, Biotek) at 450 nm [44].

Growth on spend media

Degrader and Cross-feeder cells were cultured in Marine Broth (MB, Difco 2216) and grown overnight at 25 °C. In total, 1 ml of cell culture was centrifuged (13,000 rpm for 2 min) in a 1.5 ml microfuge tube. After discarding the supernatant, the cells were washed with 1 ml of MBL minimal medium medium without carbon source. Cells were centrifuged again and the cell pellet was resuspended in 1 ml of MBL adjusted to an 0.002 OD600. A total of 10 µl of cell culture was added to the 190 µl cell free supernatant described above. Cultures were grown in a plate reader (Eon, BioTek) at 25 °C. Cell free supernatants after this growth assay were generated by sterile filtering cultures using a multi-well filter plate (AcroPrep) into a fresh 96 well plate. These supernatants were used as described above to measure acetate levels after growth on spend media.

DATA AVAILABILITY

All curated image analysis datasets and source data for figures have been uploaded to the Zenodo data repository and will be made available upon publication. https://doi.org/10.5281/zenodo.6979866.

REFERENCES

1. Corno G, Salka I, Pohlmann K, Hall AR, Grossart HP. Interspecific interactions drive chitin and cellulose degradation by aquatic microorganisms. Aquat Micro Ecol. 2015;76:27–37.
2. Graham EB, Knelman JE, Schindlbacher A, Siciliano S, Breulmann M, Yannarell A, et al. Microbes as engines of ecosystem function: when does community structure enhance predictions of ecosystem processes? Front Microbiol. 2016;7:214.
3. Henrissat B, Davies G. Structural and sequence-based classification of glycoside hydrolases. Curr Opin Struct Biol. 1997;7:637–44.
4. Kögel-Knabner I. The macromolecular organic composition of plant and microbial residues as inputs to soil organic matter. Soil Biol Biochem. 2002;34:139–62.
5. Datta MS, Sliwerska E, Gore J, Polz MF, Cordero OX. Microbial interactions lead to rapid micro-scale successions on model marine particles. Nat Commun. 2016;7:1–7.
6. Smith DC, Simon M, Alldredge AL, Azam F. Intense hydrolytic enzyme activity on marine aggregates and implications for rapid particle dissolution. Nature. 1992;359:139–42.
7. Beier S, Bertilsson S. Bacterial chitin degradation—mechanisms and ecophysiological strategies. Front Microbiol. 2013;4:149.
8. Jagmann N, Brachvogel HP, Philipp B. Parasitic growth of pseudomonas aeruginosa in co-culture with the chitinolytic bacterium Aeromonas hydrophila. Environ Microbiol. 2010;12:1787–802.
9. D'Souza G, Shitut S, Preussger D, Yousif G, Waschina S, Kost C. Ecology and evolution of metabolic cross-feeding interactions in bacteria. Nat Prod Rep. 2018;35:455–88.
10. Seth EC, Taga ME. Nutrient cross-feeding in the microbial world. Front Microbiol. 2014;5:350.
11. Morris BE, Henneberger R, Huber H, Moissl-Eichinger C. Microbial syntrophy: interaction for the common good. FEMS Microbiol Rev. 2013;37:384–406.
12. Wintermute EH, Silver PA. Emergent cooperation in microbial metabolism. Mol Syst Biol. 2010;6:407.
13. Smith P, Schuster M. Public goods and cheating in microbes. Curr Biol. 2019;29:R442–7.
14. Estrela S, Trisos CH, Brown SP. From metabolism to ecology: cross-feeding interactions shape the balance between polymicrobial conflict and mutualism. Am Nat. 2012;180:566–76.
15. Bellamy DJ, Clarke PH. Application of the second law of thermodynamics and Le Chatelier's principle to the developing ecosystem. Nature. 1968;218:1180.
16. Luli GW, Strohl WR. Comparison of growth, acetate production, and acetate inhibition of Escherichia coli strains in batch and fed-batch fermentations. Appl Environ Microbiol. 1990;56:1004–11.
17. Lilja EE, Johnson DR. Segregating metabolic processes into different microbial cells accelerates the consumption of inhibitory substrates. ISME J. 2016;10:1568–78.
18. Griffin AS, West SA, Buckling A. Cooperation and competition in pathogenic bacteria. Nature. 2004;430:1024–7.
19. Thattai M, Van Oudenaarden A. Stochastic gene expression in fluctuating environments. Genetics. 2004;167:523–30.
20. Hunt DE, Gevers D, Vahora NM, Polz MF. Conservation of the chitin utilization pathway in the Vibrionaceae. Appl Environ Microbiol. 2008;74:44–51.
21. Wang P, Robert L, Pelletier J, Dang WL, Taddei F, Wright A, et al. Robust growth of Escherichia coli. Curr Biol. 2010;20:1099–103.
22. Hockenberry AM, Micali G, Takacs G, Weng J, Hardt WD, Ackermann M. Microbiota-derived metabolites inhibit Salmonella virulent subpopulation development by acting on single-cell behaviors. PNAS. 2021;118:1–7.
23. Moreno-Gámez S, Kiviet DJ, Vulin C, Schlegel S, Schlegel K, van Doorn GS, et al. Wide lag time distributions break a trade-off between reproduction and survival in bacteria. PNAS. 2020;117:18729–36.
24. Potvin-Trottier L, Luro S, Paulsson J. Microfluidics and single-cell microscopy to study stochastic processes in bacteria. Curr Opin Microbiol. 2018;43:186–92.
25. Bakshi S, Leoncini E, Baker C, Cañas-Duarte SJ, Okumus B, Paulsson J. Tracking bacterial lineages in complex and dynamic environments with applications for growth control and persistence. Nat Microbiol. 2021;6:783–91.
26. Enke TN, Datta MS, Schwartzman J, Cermak N, Schmitz D, Barrere J, et al. Modular assembly of polysaccharide-degrading marine microbial communities. Curr Biol. 2019;29:1528–35.
27. Pontrelli S, Szabo R, Pollak S, Schwartzman J, Ledezma-Tejeida D, Cordero OX, et al. Metabolic cross-feeding structures the assembly of polysaccharide degrading communities. Sci Adv. 2022;8:eabk3076.
28. Solopova A, van Gestel J, Weissing FJ, Bachmann H, Teusink B, Kok J, et al. Bet-hedging during bacterial diauxic shift. PNAS. 2014;111:7427–32.
29. Salvy P, Hatzimanikatis V. Emergence of diauxie as an optimal growth strategy under resource allocation constraints in cellular metabolism. PNAS. 2021;118:e2013836118.
30. Amarnath K, Narla AV, Pontrelli S, Dong J, Caglar T, Taylor BR, et al. Stress-induced cross-feeding of internal metabolites provides a dynamic mechanism of microbial cooperation. bioRxiv. 2021.
31. Lin J, Amir A. From single-cell variability to population growth. Phys Rev E. 2020;101:012401.
32. Dal CA, Ackermann M, van Vliet S. Metabolic activity affects the response of single cells to a nutrient switch in structured populations. J R Soc Interface. 2019;16:20190182.
33. Kiviet DJ, Nghe P, Walker N, Boulineau S, Sunderlikova V, Tans SJ. Stochasticity of metabolism and growth at the single-cell level. Nature. 2014;514:376–9.
34. Pollak S, Gralka M, Sato Y, Schwartzman J, Lu L, Cordero OX. Public good exploitation in natural bacterioplankton communities. Sci Adv. 2021;7:eabi4717.
35. Dal CA, van Vliet S, Kiviet DJ, Schlegel S, Ackermann M. Short-range interactions govern the dynamics and functions of microbial communities. Nat Ecol Evol. 2020;4:366–75.
36. Dal CoA, Van Vliet S, Ackermann M. Emergent microscale gradients give rise to metabolic cross-feeding and antibiotic tolerance in clonal bacterial populations. Philos Trans R Soc B. 2019;374:20190080.
37. Mathis R, Ackermann M. Response of single bacterial cells to stress gives rise to complex history dependence at the population level. PNAS. 2016;113:4224–9.

38. Moreno-Gámez S, Dal Co A, van Vliet S, Ackermann M. Microfluidics for single-cell study of antibiotic tolerance and persistence induced by nutrient limitation. Methods Mol. Biol. 2021;2357:107.
39. D'Souza GG, Povolo VR, Keegstra JM, Stocker R, Ackermann M. Nutrient complexity triggers transitions between solitary and colonial growth in bacterial populations. ISME J. 2021;15:2614–26.
40. Sommer C, Straehle C, Kothe U, Hamprecht FA. Ilastik: interactive learning and segmentation toolkit. In: 2011 IEEE International Symposium on biomedical imaging: from nano to macro. IEEE; 2011. p. 230–3.
41. Kuznetsova A, Brockhoff PB, Christensen RHB. lmerTest package: tests in linear mixed effects models. J Stat Softw. 2017;82:1–26.
42. Hothorn T, Bretz F, Westfall P. Simultaneous inference in general parametric models. Biometrical J. 2008;50:346–63.
43. Drewnowska JM, Fiodor A, Barboza-Corona JE, Swiecicka I. Chitinolytic activity of phylogenetically diverse *Bacillus cereus* sensu lato from natural environments. Syst Appl Microbiol. 2020;43:126075.
44. Mai-Gisondi G, Master ER. Colorimetric detection of acetyl xylan esterase activities. In: Protein-carbohydrate interactions. New York, NY: Humana Press; 2017. p. 45–57.

ACKNOWLEDGEMENTS

We thank Ben Roller and Mateus de Oliveira Negreiros for help with the initial data analysis. Alma Dal Co and Susan Schlegel for providing scripts for image analysis; Gabriele Micali, Guga Goram, and Glen D'Souza for discussions and advice on analysis of data; Daan Kiviet for designing the microfluidic growth devices; We also thank the members of the Simons Foundation Collaboration on Principles of Microbial Ecosystems collaboration for feedback on the project.

AUTHOR CONTRIBUTIONS

MD conceived the research along with MA. MD designed and performed all experiments. SvV developed the algorithms to compute single-cell growth dynamics from the cell segmentation pipeline. MD analyzed the data with inputs from SvV and MA. MD wrote the manuscript with inputs from SvV and MA.

FUNDING

MD and MA were supported by the Simons Foundation Collaboration on Principles of Microbial Ecosystems (PriME #542389 and #542395), Swiss National Science Foundation grant 31003A_169978 and by ETH Zurich and Eawag. SvV was supported by Swiss National Science Foundation Ambizione grant PZ00P3_202186. Open access funding provided by Swiss Federal Institute of Technology Zurich.

COMPETING INTERESTS

The authors declare no competing interests.

ADDITIONAL INFORMATION

Supplementary information The online version contains supplementary material available at https://doi.org/10.1038/s41396-022-01312-w.

Correspondence and requests for materials should be addressed to Michael Daniels.

Reprints and permission information is available at http://www.nature.com/reprints

Publisher's note Springer Nature remains neutral with regard to jurisdictional claims in published maps and institutional affiliations.